Electronic structure and structural stability of TiC_xN_{1-x} alloys

Seung-Hoon Jhi and Jisoon Ihm
Department of Physics and Center for Theoretical Physics, Seoul National University, Seoul 151-742, Korea
(Received 15 July 1997)

We have investigated the structural stability and elastic stiffness of TiC_xN_{1-x} alloys using the *ab initio* pseudopotential total-energy method. Our calculation of the formation energy indicates that the alloy is stable in the whole range of the carbon concentration x and the maximum stability is obtained for $0.5 \lesssim x \lesssim 0.75$. The bulk modulus increases as nitrogen atoms replace carbon atoms and starts to saturate when the nitrogen concentration exceeds 0.5. Trends in the formation energy and bulk modulus are explained in terms of the detailed electronic structure of titanium carbonitride. Calculated results are in good agreement with available experimental data. [S0163-1829(97)00745-5]

I. INTRODUCTION

Transition-metal carbides and nitrides have recently attracted much attention due to their extraordinary mechanical and physical properties, e.g., high hardness, high melting points, and wear and corrosion resistance. Many theoretical works have been devoted to the investigation of their properties in connection with electronic structure and bonding characteristics. Previous works implied that the cohesion and the structural stability could be characterized by the average number of valence electrons per atom and the rigid-band model.[1–3] In a series of calculations of transition-metal carbides and nitrides, Häglund *et al.*,[4] showed that the cohesive energy has the largest value when the average number of valence electrons per atom (n_e) is 4 and decreases as n_e deviates from this value. For example, in the first-row transition-metal compounds, TiC was shown to have the largest cohesive energy and the replacement of carbon by nitrogen or titanium by vanadium decreased the cohesive energy. If the rigid-band model is applicable to alloy systems, it is possible to design systems with the maximal stability (i.e., the largest cohesive energy) by tuning the average electron number density appropriately. This assumption can be verified by accurate calculation on alloy systems. Experimentally, there has been much effort to improve the mechanical properties and stability of the system by alloying metal-metal or nonmetal-nonmetal elements. For the case of TiC which is regarded as a potential replacement of tungsten carbides for a cutting tool material, it has been known that alloying with TiN improves mechanical properties such as hardness, ductility, and phase stability. It has been reported that the TiC_xN_{1-x} alloy is stable in a wide range of carbon concentration and even the hardness of TiC_xN_{1-x} improves with $\sim 50\%$ of nitrogen concentration although the hardness of TiN itself is lower than that of TiC.[5,6]

In this paper, we report the electronic structure and material properties of titanium carbonitride alloy in various structures with a varying carbon concentration. Calculations have been done using the plane-wave-based *ab initio* pseudopotential method within the local-density approximation (LDA). The results indicate that the trends in the formation energy and bulk modulus as the carbon concentration x varies are closely correlated with the electronic structure of the alloy. We present the computational methods in Sec. II, the calculational results and analysis in Sec. III, and the concluding remarks in Sec. IV.

II. COMPUTATIONAL METHOD

We perform the self-consistent pseudopotential total-energy calculations with the plane-wave basis set.[7] We employ the LDA to the density functional theory. Pseudopotentials are generated semirelativistically for Ti and nonrelativistically for C and N through the Troullier-Martins scheme[8] and cast into a fully nonlocal form as suggested by Kleinman and Bylander.[9] The cutoff energy for the plane-wave basis is 56 Ry which gives the total-energy convergence within 1 mRy. We adopt the Ceperly-Alder-type exchange-correlation potential[10] as parametrized by Perdew and Zunger.[11] The Brillouin zone is sampled using the Monkhorst-Pack special point method[12] with 60 **k** points in the irreducible part of the Brillouin zone for the total-energy calculation. Atomic positions and structural parameters are fully relaxed until the Hellmann-Feynman force and the difference between stress components are reduced to less than 5 mRy/a_B and 5×10^{-2} mRy/a_B^3, respectively.

III. RESULTS

A. Cohesive properties

We are specifically interested in the formation energy defined as

$$E_{\text{form}}(x) = E_{\text{TiC}_x\text{N}_{1-x}} - xE_{\text{TiC}} - (1-x)E_{\text{TiN}}, \qquad (1)$$

as a function of the carbon concentration. Since the plane-wave basis always presumes periodic systems, we use the supercell method with the configuration of $Ti_4C_nN_{4-n}$ ($n=0$, 1, 2, 3, and 4) in order to simulate alloys. Figure 1 shows the supercell configurations for alloys ($n=1$,2, and 3) used in our calculation with only sublattice sites of nonmetal atoms shown [metal (Ti) atoms reside at the other sublattice sites of the NaCl structure]. Atomic relaxations are very small (the maximum atomic displacement is 0.032 Å in the CH structure) and not shown in the figure. Structural notations are quoted from Ref. 13.

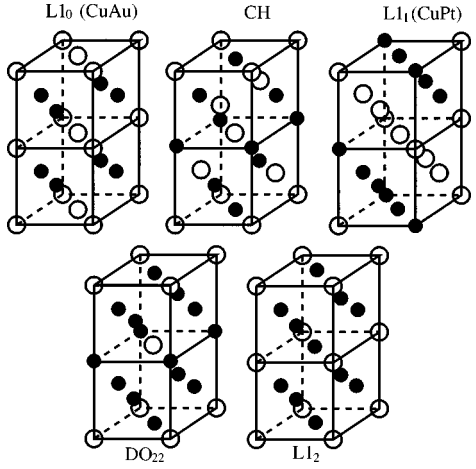

FIG. 1. Supercell configuration of TiC_xN_{1-x}. Only nonmetal (C or N) atomic sites are indicated in filled or open circles for clarity. First three structures are for $x=0.5$ and the last two are for $x=0.75$ (or, equivalently, 0.25). Structural notations follow the *structurbereicht* symbols in Ref. 13.

Figure 2 shows the results of our calculation of the formation energy. The negative formation energy for the entire concentration range at $T=0$ indicates that it is energetically favorable for TiC and TiN to mix and form alloys in agreement with experiment.[14,15] The formation energy for a given concentration differs depending on structures and has an appreciable variation at $x=0.5$. The curve obtained by polynomial fitting to our calculation has a rather asymmetric shape and shows that the TiC_xN_{1-x} alloy has the maximal stability at $x\sim0.75$. The maximum absolute value of the formation energy at $T=0$ is ~3.5 mRy at the carbon concentration $x=0.75$. However, the difference of the formation energy between $L1_2$ ($x=0.75$) and CH ($x=0.5$) structures is less than 0.3 mRy, nearly comparable to the error bar of our calculation. As most experiments are performed well above room temperature, where the contribution of the entropy to the free energy is significant, the TiC_xN_{1-x} alloy would be even more stable at finite temperatures. The maximum stability occurs in the range of $0.5<x<0.75$ under such conditions. [Assuming random distribution of carbon and nitrogen atoms, the entropic contribution ($-TS$) lowers the free energy of the $x=0.5$ alloy by ~0.3 mRy relative to that of $x=0.75$ at the room temperature.] The structural dependence of the formation energy observed above is probably obliterated by the entropy term above the room temperature and the alloy is likely to be random. Our calculations do not show a miscibility gap in any case.

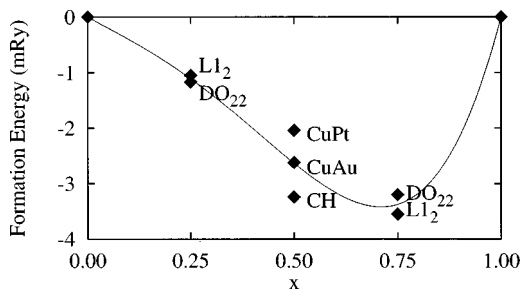

FIG. 2. Calculated formation energy of TiC_xN_{1-x} for various structures and x's at $T=0$. The solid curve is a polynomial fitting to the data points for a guide to eyes.

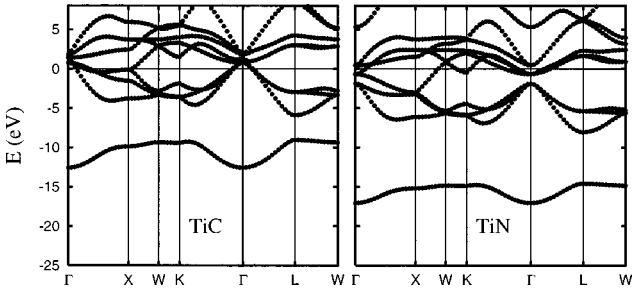

FIG. 3. The band structures of TiC and TiN. The Fermi level lies at the energy zero in each case.

We have found that the cohesive properties and the formation energy of the alloy are closely related with the electronic structures of TiC and TiN (Fig. 3). The lowest valence band is derived from the nonmetal s electrons. TiN has a lower band energy and a smaller bandwidth than TiC due to a greater electronegativity of nitrogen than carbon. The top of the valence band of TiC or TiN is mainly derived from strong covalent bonding between Ti $3d$ orbitals of e_g symmetry (i.e., x^2-y^2 and $3z^2-r^2$) and C or N $2p$ orbitals and the conduction band is in large part derived from the weak σ bonding between next-nearest-neighbor metal atoms. Some differences in band splitting and order near the Fermi level are due to the different bond strength of Ti-C and Ti-N. The Fermi level of TiC lies 0.7 eV below the valence-band maximum at the Γ point in Fig. 3. As nitrogen atoms replace carbon atoms, extra electrons from nitrogen atoms fill the unoccupied bonding states lying just above the Fermi level of TiC. The energy gain of mixing two compounds will presumably be maximum at the concentration of completely filling the bonding states. The integrated total density of states of TiC up to the aforementioned band maximum at the Γ point gives the electron number $\sim$ 8.26 corresponding to the carbon concentration $x\simeq0.74$. This simple argument agrees well with the results of the maximum absolute value of the formation energy at $x=0.75$.

As nitrogen concentration increases over 25%, additional electrons from nitrogen begin to fill the states of metal d bands mainly with the t_{2g} symmetry (i.e., xy, yz, and zx). In this regime ($x\lesssim0.75$), the trends in formation energy turn out to be dependent on the details of the electronic structure and a rather careful analysis is required as presented below. In order to specify the bonding character precisely, we investigate the density of states (DOS) and the site-projected partial density of states (SPPDOS) as plotted in Fig. 4.[16] Figure 4 shows that the metal d orbitals of t_{2g} symmetry in TiC appear predominantly above the Fermi level. In contrast to clearly observable splitting between antibonding and bonding states of e_g symmetry above and below the Fermi level, there are no pronounced features in the SPPDOS of t_{2g} symmetry that sharply distinguish the bonding and antibonding states. Three d orbitals of a Ti atom with the t_{2g} symmetry point to the 12 next-nearest-neighbor Ti atoms and make weak σ bonds with them. The charge-density plot of a state above the Fermi level in Fig. 5 shows such weak bonds as expected. If the extra electron contributed from nitrogen

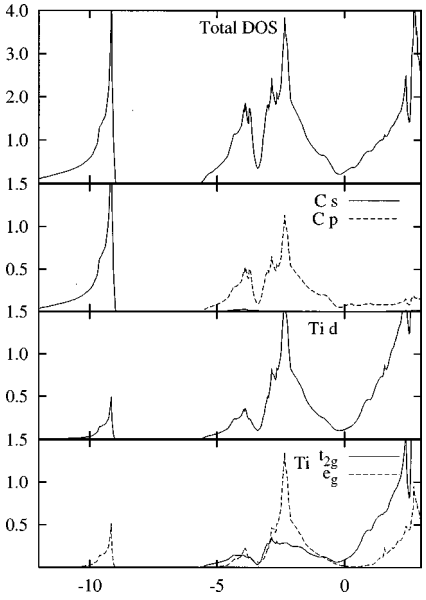

FIG. 4. Total density of states and the symmetry decomposition of the site-projected partial density of states of TiC. The Fermi level lies at the energy zero.

occupies this state, the energy gain will be very small. When the two compounds are mixed to make an alloy, the band splitting gets complicated due to the lowered symmetry, different electronegativity, and the different number of valence electrons between carbon and nitrogen. Strong $pd\sigma$ bonding states and weak metallic bonding states coexist near the Fermi level. This gives a rather slow change of the formation energy in x from 0.75 down to 0.5. In this regime, the rigid-band model may not give an accurate description of the cohesive properties of the alloy system. Relatively large differences in cohesive energy among different structures at $x=0.5$ also indicate that detailed band structures and bonding characters are important for a precise analysis of cohesive properties of the alloy. As x decreases well below 0.5, the bonding character near the Fermi level approaches that of TiN (very weak bonding or nonbonding between metal atoms) unambiguously and the magnitude of the formation energy drops to zero rapidly.

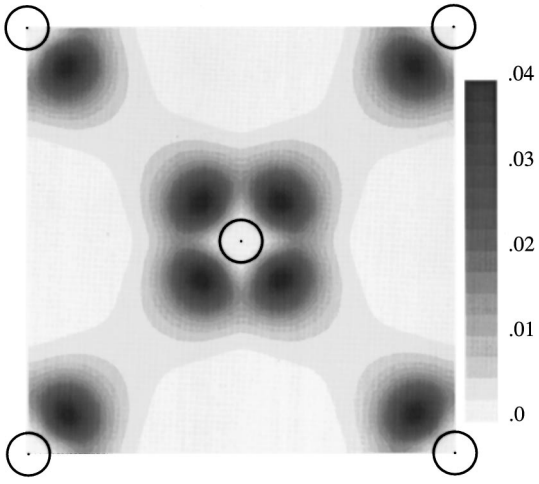

FIG. 5. Charge density of a state of TiC in the (100) plane with **k** lying in the middle of the Γ-L line. The energy eigenvalue of this state is 1.46 eV above the Fermi level. The atomic sites of Ti atoms are indicated in open circles. Weak dd bonding with the t_{2g} symmetry shows up. The unit is electrons/a_B^3.

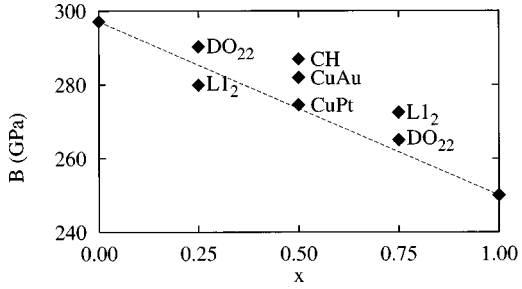

FIG. 6. Bulk modulus of TiC_xN_{1-x}. Dashed line is the linear interpolation between the bulk modulus of TiN and TiC. Deviation from the linear interpolation is significant for $0.5 \leqslant x \leqslant 0.75$.

There have been relatively few theoretical works on the TiC_xN_{1-x} alloy to our knowledge. Zhukov *et al.*[15] performed similar calculations to ours using the linear muffin-tin orbital method. The sign of the formation energy in their calculation agrees with ours, but the magnitude and the position of the maximum formation energy exhibit discrepancies. The maximum value of the formation energy reported in Ref. 15 occurs at $x=0.25$ with the magnitude of ~ 13 mRy, approximately 4 times our maximum value at $x=0.75$. Our calculated cohesive energies of bulk TiC and TiN are 1.292 and 1.216 Ry, respectively, compared with experimental values of 1.04 and 0.97 Ry.[17] As expected for an LDA calculation in general, the present calculation overestimates the cohesive energy, but the calculated difference in energy (0.078 Ry) is in excellent agreement with experiment (~ 0.07 Ry).

B. Bulk modulus

Hardness is one of the most important issues in the study of the TiC_xN_{1-x} alloy. Hardness involves the plastic deformation of materials which in turn depends critically on the motion of dislocations. Fully quantum- mechanical calculations of such properties are extremely difficult even with the state-of-the-art computational schemes and facilities. In the present work, we will confine ourselves to the study of the elastic stiffness, namely, the bulk modulus of the alloy which is feasible within the *ab initio* pseudopotential method. We caution the reader that the bulk modulus, which is often regarded as a measure of hardness of materials, is not always positively correlated with the experimentally measured hardness. TiN has a larger bulk modulus than TiC but its hardness is lower than that of TiC. With this caveat, we calculate the bulk modulus of each structure by fitting the total energy-volume curve to the Birch-Murnaghan's equation of state[18] and present the results in Fig. 6. The calculated equilibrium volume of the TiC_xN_{1-x} alloy almost obeys the Vegard's law $[V_{eq}(x)=xV_{eq}^{TiC}+(1-x)V_{eq}^{TiN}]$. The lattice constants of TiC and TiN are obtained to be 4.332 and 4.261 Å, respectively, in good agreement with experimental values of 4.33 and 4.24 Å.[17] The calculated bulk moduli of TiC and TiN are 250 and 297 GPa, respectively.[19] These values agree well with the experimental values of 240 and 318 GPa for TiC (Ref. 20) and TiN (Ref. 21) with the error of ~ 4 and $\sim 7\%$,

respectively. The bulk modulus of the alloy increases as nitrogen replaces carbon. We note that the *deviation* of the bulk modulus from the average value $[B_{av}(x)=xB_{TiC}+(1-x)B_{TiN}]$ is approximately proportional to the formation energy, having a large value at $0.5\leqslant x\leqslant 0.75$ and almost vanishes (i.e., the calculated value agrees with the linear interpolation curve in the figure) for $x=0.25$. This is partly explained by the electronic structures near the Fermi level of TiC and TiN. TiN has a greater bulk modulus than TiC simply because TiN has one *more* electron in a *smaller* unit-cell volume. The bulk modulus should obviously increase as the carbon concentration x decreases. The question is how effectively the extra electrons from nitrogen atoms in the TiC_xN_{1-x} alloy contribute to the enhancement of the bulk modulus. Those additional electrons occupy the metal $3d$ bands of t_{2g} symmetry if x is well below 0.5 as mentioned in the description of the formation energy above. Since these d electrons are relatively weakly bonded compared to $pd\sigma$ bonds involving d electrons with the e_g symmetry, the contribution of these d electrons to the bulk modulus will be smaller than that of electrons occupying the main valence bands below. However, no direct experimental data are available on the bulk modulus of TiC_xN_{1-x} for $0<x<1$ to be compared with our results. More experiments are desirable to completely reveal the elastic properties of the TiC_xN_{1-x} alloy.

IV. CONCLUSION

In summary, we have investigated the phase stability and bulk modulus of the TiC_xN_{1-x} alloy through the *ab initio* pseudopotential calculation. Our results show that the alloy is stable in the whole range of the carbon concentration and its bulk modulus increases as the nitrogen concentration increases. The maximal stability is obtained for carbon concentration $0.5\lesssim x\lesssim 0.75$. When x decreases to less than 0.5, the bulk modulus starts to saturate and the formation energy decreases rapidly. By examining the bonding characters of states near the Fermi level of TiC and TiN, we explain these trends in terms of filling the $pd\sigma$ bonding states between metal and nonmetal nearest neighbors first and then filling the weak $dd\sigma$ bonding states between next-nearest-neighbor metal atoms next as the number of electrons increases.

ACKNOWLEDGEMENTS

We thank Shinwoo Kang of SNU for helpful discussion and advice. This work is supported by the BSRI Program of the Ministry of Education and the Korea Science and Engineering Foundation through the SRC program.

[1] D. G. Pettifor, J. Phys. C **3**, 367 (1970).
[2] H. L. Skriver, Phys. Rev. B **31**, 1909 (1985).
[3] A. Fernández Guillermet and G. Grimvall, Phys. Rev. B **409**, 10 582 (1993).
[4] J. Häglund, A. Fernández Guillermet, G. Grimvall, and M. Körling, Phys. Rev. B **48**, 11 685 (1993), and references therein.
[5] V. Richter, A. Beger, J. Drobniewski, I. Endler, and E. Wolf, Mater. Sci. Eng. A **209**, 353 (1996).
[6] H. Holleck, J. Vac. Sci. Technol. A **4**, 2661 (1986).
[7] J. Ihm, A. Zunger, and M. L. Cohen, J. Phys. C **12**, 4409 (1979).
[8] N. Troullier and J. L. Martins, Phys. Rev. B **43**, 1993 (1991).
[9] L. Kleinman and D. M. Bylander, Phys. Rev. Lett. **48**, 1425 (1982).
[10] D. M. Ceperley and B. J. Alder, Phys. Rev. Lett. **45**, 566 (1980).
[11] J. P. Perdew and A. Zunger, Phys. Rev. B **23**, 5048 (1981).
[12] H. J. Monkhorst and J. D. Pack, Phys. Rev. B **13**, 5188 (1976).
[13] Z. W. Lu, S.-H. Wei, A. Zunger, S. Frota-Pessoa, and L. G. Ferreira, Phys. Rev. B **44**, 512 (1991).
[14] D. V. Shtanskii, E. A. Levashov, V. I. Kosyanin, N. B. D'yakonova, and I. V. Lyasotskii, Phys. Met. Metallogr. **80**, 560 (1995).
[15] V. P. Zhukov, V. A. Gubanov, O. Jepsen, N. E. Christensen, and O. K. Andersen, Philos. Mag. B **58**, 139 (1988), and references therein.
[16] The DOS of TiN looks very similar to that of TiC in overall shape and is not shown here. The only differences are that the Fermi level of TiN is higher than that of TiC by ~ 2 eV and the N-$2s$ peak lies about 6 eV below the C-$2s$ peak.
[17] V. P. Zhukov, V. A. Gubanov, O. Jepsen, N. E. Christensen, and O. K. Andersen, J. Phys. Chem. Solids **49**, 841 (1988), and references therein.
[18] F. Birch, J. Geophys. Res. **57**, 227 (1952).
[19] We also calculated the elastic stiffness constants c_{11} and c_{12} using the stress-strain relation. They are 513.4 and 130.2 for TiC, and 635.5 and 157.7 for TiN, respectively (all in GPa). From the relation, bulk modulus $=(c_{11}+2c_{12})/3$, we get 258 and 317 for the bulk moduli of TiC and TiN, respectively. These values are in slightly better agreement with experiment than those obtained from fitting the total energy to the Birch-Murnaghan′s equation. However, the calculation of elastic stiffness constants is believed to converge more slowly in the plane-wave-based pseudopotential method and we follow the standard practice of presenting the result from the fitting to the Birch-Murnaghan's equation in the text.
[20] R. Chang and L. J. Graham, J. Appl. Phys. **37**, 3778 (1966).
[21] J. O. Kim, J. D. Achenbach, P. B. Mirkarimi, M. Shinn, and S. A. Barnett, J. Appl. Phys. **72**, 1805 (1992).